

# Footprints of Super-GZK Cosmic Rays in the Pilliga State Forest

Luis Anchordoqui and Haim Goldberg

*Department of Physics, Northeastern University, Boston, MA 02115*

High energy cosmic ray data collected by the SUGAR Collaboration in the Pilliga State Forest have been re-analyzed using up-to-date shower simulations. Complete, inclined angle, Monte Carlo simulations reveal 2 events with energies in excess of  $7 \times 10^{19}$  eV at 95%CL, independent of the choice of hadronic interaction model and of chemical composition of the primary. An additional 3 events, with mean energy  $\gtrsim 7 \times 10^{19}$  eV, were also re-analyzed in the same manner. A lower bound on the flux at the high end of the spectrum, as observed in the Southern sky, is presented on the basis of our analysis.

NUB-3241-TH-03

## INTRODUCTION

In the mid-60's Greisen, Zatsepin, and Kuzmin (GZK) pointed out that if cosmic rays originate at cosmological distances, standard physics implies there would be an ultra violet cutoff in the observed spectrum [1]. Due to a lack of knowledge of the primary species, nowadays there is some ambiguity in the definition of the GZK energy limit. Gamma-rays produce electromagnetic cascades and for extragalactic magnetic fields  $\mathcal{O}(\text{nG})$  the high energy component of the spectrum is dramatically depleted. The net effect of proton interactions would be a pile-up around  $5 \times 10^{19}$  eV with the spectrum dropping sharply thereafter. Nucleus photodisintegration is particularly important at energies which excite the giant dipole resonance, yielding a cutoff which is species-dependent and is slightly shifted to higher energies [2]. With this in mind, in this work we consider an event to supersede the cutoff if its lower energy limit at the 95% CL exceeds  $7 \times 10^{19}$  eV. This conforms closely to the most conservative criteria delineated in Ref. [3].

A first hint of a puzzle surfaced in the highest energy Fly's Eye event [4] which has no apparent progenitor within the local supercluster [5]. Subsequent observations with the Akeno Giant Air Shower Array (AGASA) [6] carried strong indication that the cutoff was somehow circumvented in the absence of plausible nearby sources. Far from adding confirmation to what seemed a fascinating discovery, the recent analysis [7] of data recorded in monocular mode by the HiRes experiment has re-infused the field with uncertainty.

An analysis [8] of the combined data reported by the HiRes, the Fly's Eye, and the Yakutsk collaborations is supportive of the existence of the GZK cutoff at the  $> 5\sigma$  ( $> 3.7\sigma$ ) level. The deviation from GZK depends on the set of data used as a basis for power law extrapolation from lower energies. In additional input to this analysis, it has been recently noted [9] that there may be technical problems with the Yakutsk data collection. We have nothing further to add to this discussion, but it seems worthwhile to analyze any other independent set of data.

## SUGAR DATA REVISITED

The Sydney University Giant Air-shower Recorder (SUGAR) is the largest array ever built in the Southern hemisphere. It ceased operation in February 1979 after a life of 11 years [10]. The experiment comprised 47 detector stations located in the Pilliga State Forest (New South Wales, Australia) at latitude  $30^\circ 31' \text{ S}$ , longitude  $149^\circ 38' \text{ E}$ , and altitude 250 m above sea level. Each of these stations consisted of two  $6 \text{ m}^2$  conical liquid scintillator tanks separated by 50 m and buried under  $1.5 \pm 0.3$  m of earth to shield against the electromagnetic component of the shower [11]. A minimum ionizing muon traversing the scintillator produced an average of 10 photoelectrons, which were detected by photomultiplier tubes (PMTs) looking downward at the scintillator. Each tank was equipped with discriminators whose thresholds were set to the signal size expected for 3 minimum ionizing muons. A local trigger was generated for the case of hits on both tanks within 350 ns of one another. In this work we are interest in the largest showers, which determine the high end of the spectrum (energy  $\gtrsim 7 \times 10^{19}$  eV). In order to obtain a clean sample we only analyze events with the shower zenith angle  $< 45^\circ$  and muon sizes  $> 10^8$  particles. Up to 1000 m from the core all stations in these showers gave non-zero readings and thus well determined densities can be given. We require a global trigger of 6 or more stations which did record local events, with a minimum of 8 stations triggered within a time window of  $80.5 \mu\text{s}$ . There are 2 events (serial #12420 and #6179) which survive all these cuts.

A first estimate of the shower arrival direction is made by fitting a planar shower front to the station hit times. A core search is then carried out using an iterative procedure. Next, the lateral distribution function is fitted to the observed signals in the stations. In fitting the muon density account is taken of both stations which did record local events, and those which did not. The SUGAR analysis fitted using a Fisher [12] function, which is a modified version of the Greisen [13] muon structure function with the exponent of the distant term being zenith angle

dependent,

$$\rho_\mu(r) = \mathcal{N} k(\theta) \left(\frac{r}{r_0}\right)^{-a} \left(1 + \frac{r}{r_0}\right)^{-b}. \quad (1)$$

Here,  $\mathcal{N}$  is a normalization constant,  $\theta$  is the incident zenith angle,  $r$  is the perpendicular distance from the shower axis,  $r_0 = 320$  m,  $a = 0.75$ ,  $b = 1.50 + 1.86 \cos \theta$ , and

$$k(\theta) = \frac{1}{2\pi r_0^2} \frac{\Gamma(b)}{\Gamma(2-a)\Gamma(a+b-2)}. \quad (2)$$

In our analysis, we extract the lateral distribution directly from Monte Carlo simulations of showers using AIRES 2.6.0 [14]. For all shower simulations, we specify the geographical coordinates of SUGAR to turn on the geomagnetic field library in AIRES [15]. Moreover, we discard muons with energies below the muon detection threshold of a SUGAR scintillator, or  $(0.75 \pm 0.15) \sec \theta$  GeV.

A first source of systematic uncertainties is encoded in the hadronic interaction model used to process the high energy collisions. In the eikonal model [16] of high energy hadron-hadron scattering, the unitarized cross section is written as

$$\sigma_{inel} = \int d^2\vec{b} \left(1 - \exp\left\{-2\chi_{\text{soft}}(s, \vec{b}) - 2\chi_{\text{hard}}(s, \vec{b})\right\}\right), \quad (3)$$

where the scattering is compounded as a sum of ladders via hard and soft processes through the eikonals  $\chi_{\text{hard}}$  and  $\chi_{\text{soft}}$ . The leading contenders to approximate the (unknown) cross sections at cosmic ray energies, SIBYLL [17] and QGSjet [18], share the eikonal approximation but differ in their *ansätze* for the eikonals. In both cases, the core of dominant scattering at very high energies is the parton-parton minijet cross section. In the QGSjet model, this core of the hard eikonal is dressed with a soft-pomeron preevolution factor; this amounts to take a parton distribution which is Gaussian in the transverse coordinate distance  $|\vec{b}|$ . In SIBYLL, the transverse density distribution is taken as the Fourier transform of the electric form factor, resulting in an exponential (rather than Gaussian) falloff of the parton density profile with  $|\vec{b}|$ . Some of the shower characteristics resulting from these choices are readily predictable: the harder form of the SIBYLL form factor allows a greater retention of energy by the leading particle, and hence less available for the ensuing shower [19]. This in turn explains the reduction of mean secondary multiplicity observed [20] in going from QGSjet to SIBYLL simulations. The growth in inelastic cross section saturates the  $\log^2 s$  Froissart bound in both cases, but the multiplicative constant turns out to be larger for SIBYLL, enhancing the cross section by about 30% at energies of  $10^{19-20}$  eV. However, the shower characteristics are the result of exponentially many hadronic

collisions in air, and for these the larger SIBYLL cross section is somewhat offset by its smaller multiplicity, reducing the differences between the two schemes down to the level of 10-20%. These and other properties of the two schemes have been amply displayed in a recent work [21].

Eight stations were involved in the event #12420, all with local triggers (i.e., 16 scintillators). A map of the recorded muon densities in a plane perpendicular to the shower axis was reported by the SUGAR Collaboration in Ref. [22]. The north tank of one of the stations recorded a saturated response (density  $> 800$  m $^{-2}$ ). The standard analysis of the SUGAR Collaboration placed the shower core on this tank. However, the collaboration concluded that in such a big shower saturated densities may occur at distances up to several hundred meters from the core. Moreover, for large signals, afterpulsing in the PMTs can lead to an overestimate of the muon density. The location of the core was best re-estimated by assigning lower energy densities to this station. Since the probability of recording a saturated response from an actual density less than 100 m $^{-2}$  is negligible, the SUGAR Collaboration concluded that this value of density in both tanks would yield a minimum value on the primary energy. In our analysis we adopt this conservative lower bound. Note that this second source of systematic error can lead to an underestimate of the energy. The best  $\chi^2$  fit for QGSjet01 (SIBYLL 2.1), assuming a proton primary, is given in Fig. 1 (Fig. 2). Note that AIRES + SIBYLL simulations result in an energy which exceeded the AIRES + QGSjet value by about 10%. This agrees with the analysis of the AGASA Collaboration [23].

The energy that we find for event#12420 using QGSjet is about 5% above the energy reported by the SUGAR Collaboration [10], their estimate being based on the Hillas E model [24]

$$E_{\text{SUGAR}} = 1.64 \times 10^{18} \left(\frac{N_\mu^{\text{vert}}}{10^7}\right)^{1.075} \text{ eV}. \quad (4)$$

In further exploring the energy systematics, we have generated proton vertical showers using AIRES+QGSjet and compared (in Fig. 3) the  $N_\mu^{\text{vert}} - E$  relation with that given in Eq. (4). As can be seen from Fig. 3, this conversion formula underestimates the energy by about 25%, for a given  $N_\mu^{\text{vert}}$ , when compared with our simulations. However, as noted above, the overall underestimate of the SUGAR assignment for the energy from our best fit is about 5%. This is readily explained by noting that the normalization constant  $\mathcal{N}$  (used by the SUGAR Collaboration as the muon size) and obtained through the fit to the Fisher function overestimates the number of muons (as found through our simulation) by about 17% (see Table I). Since the equivalent vertical muon size and energy bear a near-linear relationship to one another (see Fig. 3), these systematic effects nearly offset one another, bringing the SUGAR energy estimate near to that obtained

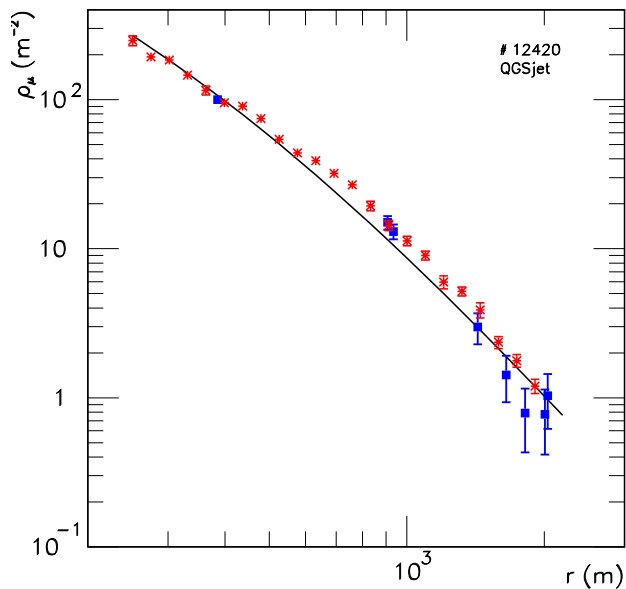


FIG. 1: Best fit to the muon density (\*) for event #12420 using AIRES + QGSjet. The estimated primary energy is  $1.1 \times 10^{20}$  eV, with  $\chi^2/\text{d.o.f.} = 9.4/7$ . The recorded particle densities as reported by the SUGAR Collaboration are indicated with squares. The solid line indicates the best fit reported by SUGAR Collaboration using the Fisher function ( $\chi^2/\text{d.o.f.} = 10.3/7$ ).

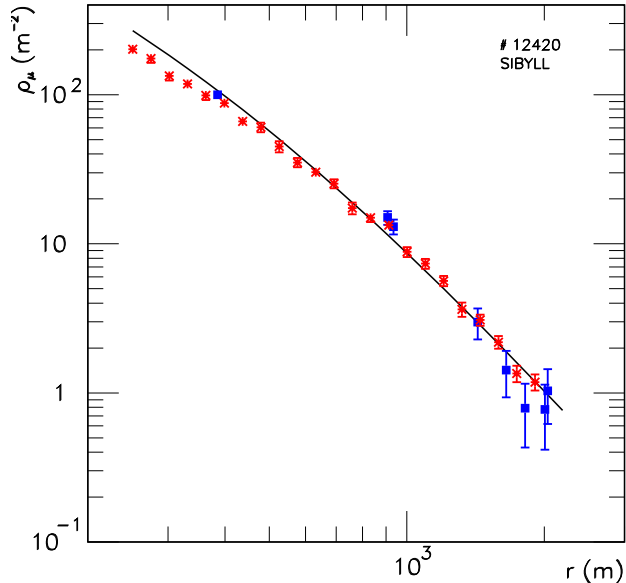


FIG. 2: Best fit to the muon density (\*) for event #12420 using AIRES + SIBYLL. The estimated energy is  $1.2 \times 10^{20}$  eV, with  $\chi^2/\text{d.o.f.} = 9.1/7$ . The recorded particle densities as reported by the SUGAR Collaboration are indicated with squares. The solid line indicates the best fit reported by SUGAR Collaboration using the Fisher function ( $\chi^2/\text{d.o.f.} = 10.3/7$ ).

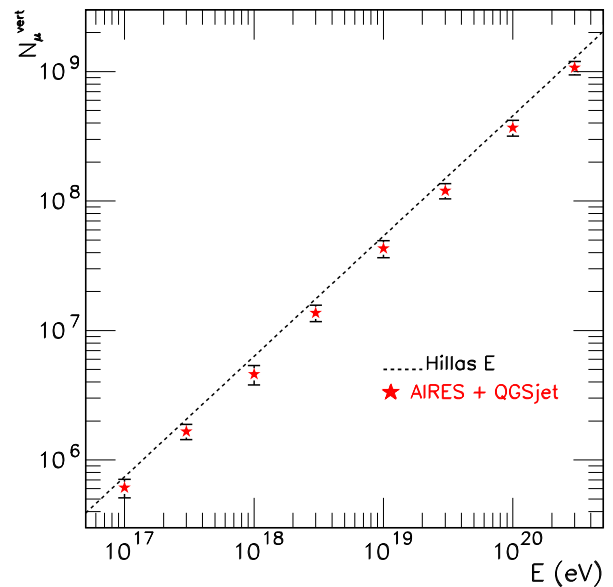


FIG. 3: Total number of muons as a function of the energy shower. The simulations were carried out with AIRES + QGSjet, assuming protons as primaries. The particles were injected vertically at the top of the atmosphere and the detector was placed at 250 m above sea level. Muons with energies below the SUGAR threshold (0.75 GeV) are not taken into account in the simulations. The dashed line indicates the Hillas parametrization (see main text).

with AIRES+QGSjet. Implicitly, this discussion supports the consistency of the constant intensity cut method of mapping muon sizes from inclined to vertical [25].

A third source of systematic uncertainty is hidden in the chemical composition. As a first approximation, a shower produced by a nucleus with energy  $E_A$  and mass  $A$  can be modeled by the collection of  $A$  proton showers, each with  $A^{-1}$  of the nucleus energy. Now, using Eq. (4) a straightforward calculation shows that the total number of muons produced by the superposition of  $A$  individual proton showers is,  $N_\mu^{\text{vert}} \propto A(E_A/A)^{0.93}$ . Consequently, one expects a cosmic ray nucleus to produce about  $A^{0.07}$  more muons than a proton. Conversely, a given muon size will imply a smaller energy for a complex nucleus. Thus, we can estimate the lower energy limit of the event #12420, by simulating several sets of showers for  $^{56}\text{Fe}$  primaries [26]. The QGSjet package was used to process the high energy hadronic interactions. Energies below  $7.0 \times 10^{19}$  eV are excluded at the 95% CL.

The analysis of the second event (#6179) is less straightforward. This is because there were stations in which one of the tanks did not fire [22]. In assigning the trigger intensity of these tanks, the SUGAR Collaboration took as a maximum the density in the firing tanks, and as a minimum the density averaged over all the tanks that were expected to fire. Data scaled to a

TABLE I: Primary energy in units of  $10^{20}$  eV for proton primaries estimated using AIRES + QGSjet. The corresponding muon sizes and normalization constant of the Fisher function are also given in units of  $10^8$  particles. The last 3 columns indicate the incident zenith angle and the arrival directions in equatorial coordinates ( $\alpha, \delta$ ) with respect to the reference system B1950 [10]. The estimated angular uncertainty for all these events is  $4.3^\circ$ .

Number	$\mathcal{N}$	$E$	$N_\mu$	$\theta$ [deg.]	$\alpha$ [deg.]	$\delta$ [deg.]
12420	3.47	1.10	$2.99 \pm 0.35$	43	147.0	-43.6
6179	4.06	1.03	$3.56 \pm 0.45$	24	121.5	-32.0
7329	2.63	0.77	$2.24 \pm 0.34$	38	135.0	04.3
1696	2.55	0.71	$2.20 \pm 0.27$	33	331.5	-32.2
6239	2.27	0.70	$1.96 \pm 0.27$	40	280.5	-55.6

muon size of  $4.5 \times 10^8$  is shown in Ref. [22]. Because of the resulting decrease in the quality of the statistics, the likelihood in this case did not converge reliably to a global minimum. However, a 95% confidence interval,  $7.0 \times 10^{19}$  eV  $< E < 1.2 \times 10^{20}$  eV, was readily obtained.

For a more extended comparison with the analysis reported by the SUGAR Collaboration, we relax the global trigger designated above, and follow several more recent analyses of SUGAR data [27] by considering events in which 5 pairs of scintillators fired within a time window of  $80.5 \mu\text{s}$ . For this kind of global trigger, the uncertainty in the arrival direction is manageable at an average of  $4.3^\circ$  [28]. (For 3- and 4-fold triggers, this rises beyond 10 degrees.) With this new global trigger, we simulate showers with AIRES + QGSjet and find that by increasing the energy reported by the SUGAR Collaboration by about 5% we reasonably conform to the lateral profiles of the events as described by the Fisher function, with normalization constants taken from [10] and given in Table I. As a result, we find 4 events (including #6179 discussed above) with energies  $> 7 \times 10^{19}$  eV. These qualitative fits are shown in Fig. 4, and the parameters characterizing these events are detailed in Table I.

A closer examination of Fig. 4 reveals a systematic deviation between the QGSjet and Fisher function lateral distribution profiles. As can be seen in Fig. 5, the divergences become more severe when SIBYLL is used to process the hadronic interactions. Of course, this comparison with the Fisher function plays no role in discriminating between these schemes.

## ENERGY SPECTRUM

The effective detecting area of the array at any time is given by the product of the active geometric surface area of the array,  $S$ , times the probability  $p(\mathcal{N}, \theta)$  that a shower falling within  $S$  will be detected,

$$A_{\text{eff}}(\mathcal{N}, \theta, t) = S(t) p(\mathcal{N}, \theta). \quad (5)$$

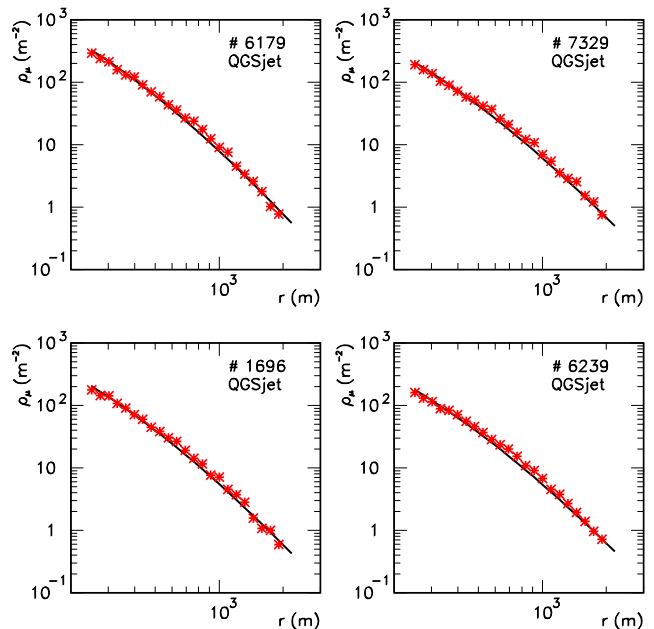


FIG. 4: Lateral distributions obtained using air-shower simulations with AIRES + QGSjet (\*) superimposed over the best fits of the Fisher function (solid line) as reported by the SUGAR Collaboration. The corresponding primary energies used in the simulations are those given in Table I.

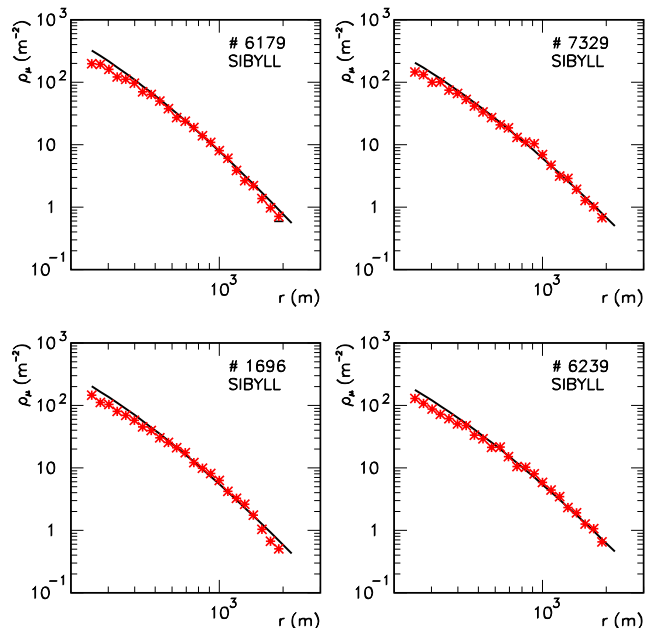


FIG. 5: Lateral distributions obtained using air-shower simulations with AIRES + SIBYLL (\*) superimposed over the best fits of the Fisher function (solid line) as reported by the SUGAR Collaboration. The corresponding primary energies in units of  $10^{19}$  eV used in the simulations are: 11.3, 8.5, 7.8, and 7.7, for #6179, #7329, #1696 and #6239, respectively.

The SUGAR Collaboration reported [29] an angle specific exposure for showers with  $\mathcal{N} = 4 \times 10^8$  and  $\theta = 32^\circ$ ,

$$\mathcal{E}(32^\circ) = \int_0^T dt S(t) p(4 \times 10^8, 32^\circ) = 540 \text{ km}^2 \text{ yr}, \quad (6)$$

where  $T = 11$  yr. This value of  $p$  was obtained by allowing a global trigger of 3 or more stations. Because the detection probability decreases with smaller muon size (as is the case for the events in Table I) and with our restriction to 5 triggers, Eq. (6) leads to an upper limit on the integrated exposure for the parameter space relevant to this study,

$$\begin{aligned} \mathcal{E}(\theta < 45^\circ) &= 2\pi \mathcal{E}(32^\circ) \int_{\sqrt{2}/2}^1 \frac{p(\theta)}{p(32^\circ)} \cos \theta d \cos \theta \\ &\approx 862 \text{ km}^2 \text{ sr yr}, \end{aligned} \quad (7)$$

where  $p(\theta) \propto \cos \theta$  is the probability of detection at zenith angle  $\theta$  [30].

The observed number of events in an energy bin  $\Delta$  is given by

$$\begin{aligned} N &= \mathcal{E} \int_{\Delta} E J(E) \frac{dE}{E} \\ &\simeq 2.3 \mathcal{E} \overline{E} J(\overline{E}) \Delta \log_{10} E, \end{aligned} \quad (8)$$

so that

$$\overline{E}^3 J(\overline{E}) = \overline{E}^2 \frac{N}{2.3 \mathcal{E} \Delta \log_{10} E}, \quad (9)$$

where  $\overline{E}$  is the value of  $E$  at the center of the logarithmic interval.

Following common practice, we adopt a bin size  $\Delta \log_{10} E = 0.1$ . As previously discussed, we have adopted a lower energy cut of  $10^{19.85}$  eV. The events listed in Table I are then grouped in two bins, and the resulting contributions to the cosmic ray spectrum as given by Eq. (9) are shown in Fig. 6. The error on the mean

$$\begin{aligned} \Delta \log_{10} [\overline{E}^3 J(\overline{E})] &= \Delta \log_{10} N \\ &= 0.343 \Delta \ln N \\ &= 0.343 \frac{\Delta N}{N}, \end{aligned} \quad (10)$$

is taken as Poisson (i.e.,  $\Delta N = \sqrt{N}$ ).

On the same figure are shown the data points for the flux as reported by the AGASA [23], Fly's Eye [31], and HiRes [7] collaborations. Also shown is the flux obtained by a recalibration of the 4 highest energy events observed at the Haverah Park facility [32]. We note that the AGASA flux plotted is taken from the most recent analysis published by the AGASA Collaboration [23], containing events with zenith angle  $< 45^\circ$ , recorded until July 2002. The energy is calibrated using an average over hadronic interaction models and primary species ( $p$  and  $^{56}\text{Fe}$ ). It is of interest to the present work that the energies obtained in this manner differ by only about 2% with respect to those obtained via ARES + QGSjet simulation.

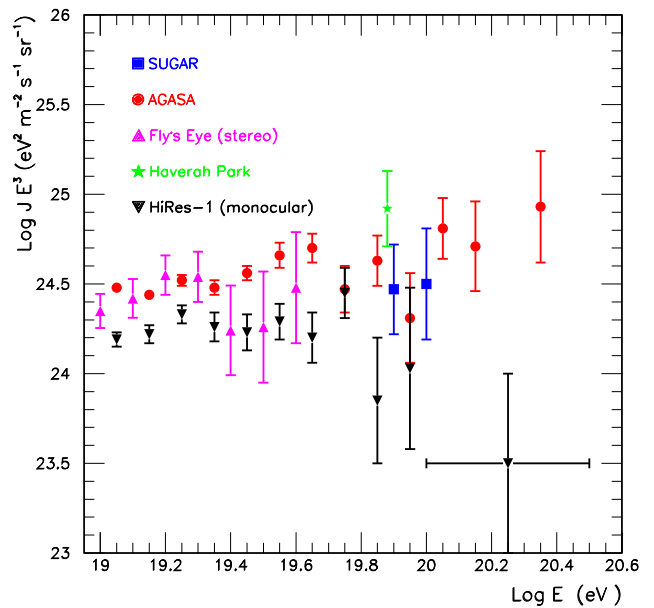


FIG. 6: Upper end of the cosmic ray energy spectrum as observed by 5 different experiments (for details see main text).

## SUMMARY AND DISCUSSION

(1) We have re-examined cosmic ray data taken over two decades ago at the SUGAR facility, using up-to-date simulation methods to describe shower evolution in the atmosphere, with resulting correlation between muon size and energy. We conclude that there is strong evidence for the existence of events superseding the GZK cutoff. Specifically, there are two events in the sample with energy  $> 7 \times 10^{19}$  eV at the 95%CL. This statement includes consideration of systematic uncertainties stemming from choice of hadronic interaction model and chemical composition.

(2) As part of our exploration of the systematics, we have compared our study with methods used by the SUGAR Collaboration for energy assignment. We found that through a compensation of errors in assessing muon size from fits to the Fisher function and the normalization of the Hillas relation [24], the final SUGAR energies are consistently about 5% below those found via ARES + QGSjet simulation. Remarkably, we find (Fig. 3) that the exponent in the power law  $N_\mu^{\text{vert}} = \mathcal{K} E^\alpha$  is consistent with Hillas's  $\alpha = 0.93$ , but with a shift in the constant  $\mathcal{K}$  upward by 25%. A detailed recent study [21] shows that in fact the exponent  $\alpha$  is more properly taken to have a logarithmic energy-dependence.

(3) Using a conservative estimate on the acceptance of the SUGAR facility, we have been able to present lower bounds on the cosmic ray flux in the case of a proton primary with QGSjet as the hadronic interaction model. This lower bound would prevail for SIBYLL inde-

pendent of the primary composition. The lower bounds would be slightly modified in the case that QGSjet successfully models the hadronic interaction at high energies and the primary composition is dominated by heavy nuclei. Within a standard deviation, our data points are consistent with both AGASA and HiRes. Because of the Southern hemisphere exposure of SUGAR, this comprises interesting support for North-South isotropy in the arrival direction of the highest energy cosmic rays.

(4) An extrapolation of our analysis to the entire SUGAR data set would involve observations using a 3 station global trigger, with its attendant loss of angular resolution beyond  $10^\circ$ . Because of the similar procedures for energy assignment in ground arrays, the consistency of the SUGAR spectrum with AGASA observations supports recent anisotropy studies [33] of low-multipole inhomogeneities that combine data taken from these 2 experiments.

(5) To give a visual impression of the Southern cosmic ray sky, in Fig. 7 we show the arrival direction of the events given in Table I together with the potential sources included in the first budget of the anisotropy search program for the Pierre Auger Observatory [34].

(6) As part of our study, we have noted an interesting differentiating signature between the QGSJET and SIBYLL models. Previous work [20] has shown that for a fixed (proton) primary energy, muon densities obtained in shower simulations using SIBYLL fall more rapidly with lateral distance to the shower core than those obtained using QGSJET. This can be understood as a manifestation of the enhanced leading particle effect in SIBYLL, which can be traced to the relative hardness of the electromagnetic form factor profile function. From Figs. (4) and (5), it is apparent that even when the energy is left as a free parameter, the curvature of the distribution ( $d^2\rho_\mu/dr^2$ ) is measurably different in the two cases, and could possibly serve as a discriminator between hadronic interaction models with sufficient statistics.

In summary, the footprints analyzed in this paper are an interesting addition to the data set, but not enough to weigh in on one side or the other with respect to the GZK question. The Pierre Auger Observatory [38] now coming on line with its superior energy resolution and statistics will supply the final verdict on the GZK cutoff.

### Acknowledgments

We would like to thank Tom McCauley, Tom Paul, and Alan Watson for valuable discussions. The work of LAA and HG has been partially supported by the US National Science Foundation (NSF), under grants No. PHY-0140407 and No. PHY-0244507, respectively.

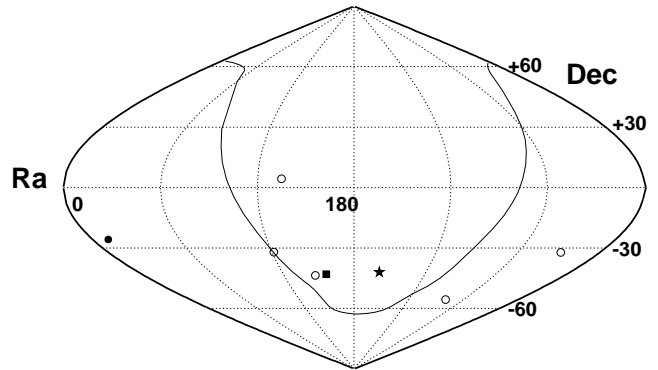


FIG. 7: Arrival direction of the events given in Table I (o) in equatorial coordinates B1950. Also shown in the figure are the position in the sky of potential cosmic ray sources: Cen A (\*) [35], NGC3256 (■) [36], and NGC253 (●) [37]. The solid line indicates the position of the Galactic plane.

- 
- [1] K. Greisen, Phys. Rev. Lett. **16**, 748 (1966); G. T. Zatsepin and V. A. Kuzmin, JETP Lett. **4**, 78 (1966) [Pisma Zh. Eksp. Teor. Fiz. **4**, 114 (1966)].
  - [2] For recent reviews see *e.g.*, P. Bhattacharjee and G. Sigl, Phys. Rept. **327**, 109 (2000) [arXiv:astro-ph/9811011]; M. Nagano and A. A. Watson, Rev. Mod. Phys. **72**, 689 (2000); L. Anchordoqui, T. Paul, S. Reucroft and J. Swain, Int. J. Mod. Phys. A **18**, 2229 (2003) [arXiv:hep-ph/0206072]; F. W. Stecker, J. Phys. G **29**, R47 (2003) [arXiv:astro-ph/0309027].
  - [3] G. R. Farrar and P. L. Biermann, Phys. Rev. Lett. **83**, 2472 (1999) [arXiv:astro-ph/9901315].
  - [4] D. J. Bird *et al.*, Astrophys. J. **441**, 144 (1995).
  - [5] J. W. Elbert and P. Sommers, Astrophys. J. **441**, 151 (1995) [arXiv:astro-ph/9410069].
  - [6] M. Takeda *et al.*, Phys. Rev. Lett. **81**, 1163 (1998) [arXiv:astro-ph/9807193].
  - [7] T. Abu-Zayyad *et al.* [High Resolution Fly's Eye Collaboration], arXiv:astro-ph/0208301. D. R. Bergman [HiRes Collaboration], Mod. Phys. Lett. A **18**, 1235 (2003) [arXiv:hep-ex/0307059].
  - [8] J. N. Bahcall and E. Waxman, Phys. Lett. B **556**, 1 (2003) [arXiv:hep-ph/0206217].
  - [9] A. A. Watson, Proc. 28th International Cosmic Ray Conference (Tsukuba), 373 (2003).
  - [10] M. M. Winn, J. Ulrichs, L. S. Peak, C. B. McCusker and L. Horton, J. Phys. G **12**, 653 (1986).
  - [11] R. G. Brownlee *et al.*, Can. J. Phys. **46**, S259 (1968).
  - [12] A. Fisher, PhD Thesis, University of Sydney (1970). See also, R. G. Brownlee *et al.*, Acta Phys. Acad. Sci. Hung. **29** Suppl. 3, 651 (1970).
  - [13] K. Greisen, Ann. Rev. Nuclear Sci. **10**, 63 (1960); S. Bennett and K. Greisen, Phys. Rev. **124**, 1982 (1961).
  - [14] S. J. Sciutto, arXiv:astro-ph/9905185; arXiv:astro-ph/0106044.
  - [15] In AIREs, the Earth's magnetic field is evaluated us-

- ing data from the International Geomagnetic Reference Field, distributed by the National Geophysical Data Center, Boulder (CO) USA, <http://www.ngdc.noaa.gov>.
- [16] R. J. Glauber and G. Matthiae, Nucl. Phys. B **21**, 135 (1970); L. Durand and H. Pi, Phys. Rev. Lett. **58**, 303 (1987).
- [17] R. S. Fletcher, T. K. Gaisser, P. Lipari and T. Stanev, Phys. Rev. D **50**, 5710 (1994).
- [18] See *e.g.*, N. N. Kalmykov, S. S. Ostapchenko and A. I. Pavlov, Nucl. Phys. Proc. Suppl. **52B**, 17 (1997).
- [19] As noted in another context, this behavior is also characteristic of the neutrino-hadron neutral current interaction. L. Anchordoqui, H. Goldberg, T. McCauley, T. Paul, S. Reucroft and J. Swain, Phys. Rev. D **63**, 124009 (2001) [arXiv:hep-ph/0011097].
- [20] L. A. Anchordoqui, M. T. Dova, L. N. Epele and S. J. Scutto, Phys. Rev. D **59**, 094003 (1999) [arXiv:hep-ph/9810384].
- [21] J. Alvarez-Muniz, R. Engel, T. K. Gaisser, J. A. Ortiz and T. Stanev, Phys. Rev. D **66**, 033011 (2002) [arXiv:astro-ph/0205302].
- [22] C. J. Bell *et al.*, J. Phys. A **7**, 990 (1974).
- [23] M. Takeda *et al.*, Astropart. Phys. **19**, 447 (2003) [arXiv:astro-ph/0209422].
- [24] A. M. Hillas, J. D. Hollows, H. W. Hunter, and D. J. Marsden, Proc. 12th International Cosmic Ray Conference (Hobart) **3**, 1007 (1971).
- [25] J. Alvarez-Muniz, R. Engel, T. K. Gaisser, J. A. Ortiz and T. Stanev, Phys. Rev. D **66**, 123004 (2002) [arXiv:astro-ph/0209117].
- [26] Because of the position of  $^{56}\text{Fe}$  on the binding energy curve, it is considered to be a significant end product of stellar evolution, and higher mass nuclei are found to be much rarer in the cosmic radiation. See *e.g.* E. M. Burbidge, G. R. Burbidge, W. A. Fowler and F. Hoyle, Rev. Mod. Phys. **29**, 547 (1957).
- [27] R. W. Clay, R. Meyhandan, L. Horton, J. Ulrich and M. M. Winn, Astron. Astrophys. **255**, 167 (1992); L. J. Kewley, R. W. Clay and B. R. Dawson, Astropart. Phys. **5** (1996) 69.
- [28] R. G. Brownlee, PhD Thesis, University of Sydney (1970).
- [29] L. Horton, C. B. A. McCusker, L. S. Peak, J. Ulrichs, and M. M. Winn, Proc. 18th International Cosmic Ray Conference (Bangalore) **6**, 124 (1983).
- [30] R. G. Brownlee, Can. J. Phys. **46**, S263 (1968).
- [31] D. J. Bird *et al.* [HIRES Collaboration], Astrophys. J. **424** (1994) 491.
- [32] M. Ave, J. Knapp, J. Lloyd-Evans, M. Marchesini and A. A. Watson, Astropart. Phys. **19**, 47 (2003) [arXiv:astro-ph/0112253].
- [33] L. A. Anchordoqui, C. Hojvat, T. P. McCauley, T. C. Paul, S. Reucroft, J. D. Swain and A. Widom, Phys. Rev. D (to be published) [arXiv:astro-ph/0305158]; G. Sigl, F. Miniati and T. Ensslin, arXiv:astro-ph/0309695.
- [34] R. W. Clay [Pierre Auger Collaboration], arXiv:astro-ph/0308494.
- [35] G. R. Farrar and T. Piran, arXiv:astro-ph/0010370; L. A. Anchordoqui, H. Goldberg and T. J. Weiler, Phys. Rev. Lett. **87**, 081101 (2001) [arXiv:astro-ph/0103043].
- [36] M. Giller, M. Wojciech, S. Andrzej, arXiv:astro-ph/0308532.
- [37] L. A. Anchordoqui, H. Goldberg and D. F. Torres, Phys. Rev. D **67**, 123006 (2003) [arXiv:astro-ph/0209546]; L. Anchordoqui, H. Goldberg, S. Reucroft and J. Swain, Phys. Rev. D **64**, 123004 (2001) [arXiv:hep-ph/0107287]; L. A. Anchordoqui, G. E. Romero and J. A. Combi, Phys. Rev. D **60**, 103001 (1999) [arXiv:astro-ph/9903145].
- [38] P. Sommers, Comments Nucl. Part. Phys. **2**, A261 (2002).